LASERS

PACS numbers: 42.55.Lt; 42.60.Lh
DOI: 10.1070/QE2004v034n10ABEH002656

Effect of the pump intensity on the efficiency of a KrF excimer electric-discharge laser on a $He-Kr-F_2$ mixture

A.M. Razhev, A.I. Shchedrin, A.G. Kalyuzhnaya, A.V. Ryabtsev, A.A. Zhupikov

***Abstract*. The effect of the pump parameters on the efficiency of operation of a KrF gas-discharge excimer laser on a $He-Kr-F_2$ mixture is studied. A theoretical model of the excitation system and the kinetic processes in the plasma of this laser is developed. A pump system based on an *LC* inverter with a spark gap as a high-voltage switch, automatic UV preionisation, and a low-inductance discharge circuit is created. To increase the efficiency and the output energy of the KrF laser based on a $He-Kr-F_2$ mixture, it is proposed to enhance the pump intensity to 4 MW cm^{-3} by increasing the inductance between the *LC* inverter and the discharge circuit to 100 nH. An output energy of 1 J at an efficiency of 2 % is achieved for the first time for the KrF laser operating on this mixture.**

Keywords: *KrF excimer laser, output energy, pump intensity, buffer gas.*

1. Introduction

Gas-discharge excimer 248-nm KrF lasers are currently widely used in microelectronics, photolithography, and medicine. From the practical point of view, the output energy and the total efficiency η are their most important parameters. The efficiency and reliability of the laser pump system, the sort of the buffer gas in the active medium that determines the cost of the gas mixture, and the charging-voltage value are also of great importance. This paper presents the results of theoretical and experimental studies of the effect of the pump intensity on the lasing efficiency of a transverse-discharge-excited KrF gas-discharge excimer laser based on a $He-Kr-F_2$ mixture. The pump intensity is defined as the specific power W of pumping the active medium expressed by the formula $W = E/V\tau$, where E is the energy stored in the peaking capacitor, V is the active volume, and τ is the base-level duration of the first half-period of the discharge current.

A KrF excimer laser on a $Ne-Kr-F_2$ mixture with a pump system based on a scheme with a discharging capacitor and automatic UV preionisation was described in [1]. An output energy of 600 mJ at $\eta = 1.6$ % was obtained at a charging voltage of 36 kV, and the maximum efficiency (2.8 %) was achieved at 300 mJ. The output energy achieved in [2] using a similar laser with the same pump system was 500 mJ at a total efficiency of 3.9 %. The laser used in [3] was similar to the latter and allowed an output energy of 810 mJ and $\eta = 2.6$ % to be attained. It was shown in [2, 3] that, to obtain high output energies and efficiencies for a KrF laser on mixtures with Ne as the buffer gas, a pump intensity of 1.8 – 2.5 MW cm^{-3} is required.

The KrF laser on a $He-Kr-F_2$ mixture was excited in [4] using a pump system similar to that described in [1, 2]. An output energy of 500 mJ at $\eta = 1.1$ % was obtained at a charging voltage of 45 kV. The maximum output energies of a KrF gas-discharge laser achieved in [5] were 5 and 4.5 J in mixtures with Ne and He as buffer gases, respectively. For this purpose, a complex pump system based on a scheme with a two-stage Marx generator was developed. It operated at charging voltages of 190 – 220 kV. The efficiency of this KrF laser calculated with respect to the energy stored in capacitors was 0.53 % and 0.47%, respectively. In [6], the same authors replaced the Marx generator by an excitation system of the *LC*-inverter type with magnetic-compression sections for exciting an active volume of 6.5 cm × 5.0 cm × 80 cm, thus allowing the charging voltage to be reduced from 192 to 65 kV. In this case where the pump intensity was 0.6 MW cm^{-3}, the lasing energy in the $Ne-Kr-F_2$ active medium decreased from 5.0 to 2.5 J, and the total efficiency increased to 2.5 %. However, since the use of He as the buffer gas under such a low pump intensity in [6] made it impossible to achieve high values of the KrF-laser output energy and efficiency, these data are not reported.

In order to achieve efficient lasing in a KrF laser on a $He-Kr-F_2$ mixture in [7], we increased the pump intensity to 3.0 MW cm^{-3}, thus allowing the output energy to be increased to 800 mJ at a total efficiency of 2.0 %.

From the papers considered, it follows that the highest KrF-laser efficiencies and output energies were attained on a $Ne-Kr-F_2$ mixture at a specific pump intensity of ~ 2 MW cm^{-3}. When He was used as the buffer gas instead of Ne, it was necessary to increase the pump intensity to 3.0 MW cm^{-3}.

The aim of this work was to study theoretically and

A.M. Razhev, A.A. Zhupikov Institute of Laser Physics, Siberian Branch, Russian Academy of Sciences, prosp. Akad. Lavrent'eva 13/3, 630090 Novosibirsk, Russia;
e-mail: razhev@laser.nsc.ru; web-site: www.laser.nsc.ru;
A.I. Shchedrin, A.G. Kalyuzhnaya, A.V. Ryabtsev Institute of Physics, National Academy of Sciences of Ukraine, prosp. Nauki 46, 03650 Kiev, Ukraine; e-mail: ashched@iop.kiev.ua; web-site: www.iop.kiev.ua

Received 25 March 2004; revision received 30 June 2004
Kvantovaya Elektronika **34** (10) 901 – 906 (2004)
Translated by A.S. Seferov

experimentally the effect of the pump intensity on the output energy and efficiency of a KrF laser on a He–Kr–F_2 mixture and also to study the methods for controlling the parameters and to develop a highly efficient pump system.

2. Experimental setup

We measured the energy and amplitude–time characteristics of the voltage, current, and radiation pulses in the nanosecond range. The instrumentation and methods for measurements are described in [8].

An equivalent electric circuit of the pump system of a KrF excimer laser (Fig. 1) consisted of storage capacitors C_1 and C_2 connected according to the circuit of an LC inverter with a spark gap R_1 as a high-voltage switch. The pump system included a device for automatic UV preionisation and a low-inductance discharge circuit formed by a capacitor C_3 and the active medium with a resistance R_3, which changed from infinity to $\sim 0.2\ \Omega$. The entire pump system thus consisted of two circuits: the LC inverter with the high-voltage switch and automatic UV preionisation (inductor L_2) and the low-inductance discharge circuit (inductor L_3).

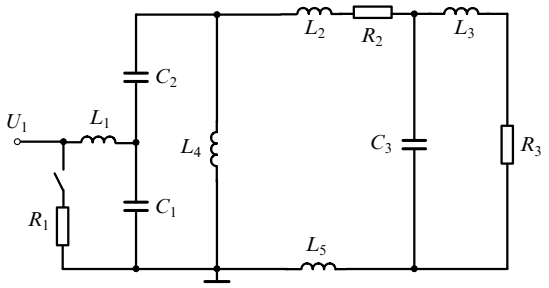

Figure 1. Equivalent electric circuit of the laser: $R_1 \sim 0.1\ \Omega$, $R_2 \sim 0.1\ \Omega$, $R_3 \sim 0.2\ \Omega$; $C_1 = 50$ nF, $C_2 = 100$ nF, $C_3 = 30$ nF; $L_1 = 40$ nH; $L_2 = 20$ nH, $L_3 = 3.8$ nH, $L_4 = 2.5$ μH, $L_5 = 30 - 100$ nH.

The main task of this study was to determine the parameters of the pump system that ensure both the maximum efficiency of the energy transfer from the storage capacitors C_1 and C_2 into C_3 of low-inductance discharge circuit and the maximum efficiency of the energy transfer from C_3 to the active gaseous medium, thus limiting the loss of this energy associated with its partial return to C_1 and C_2. It was taken into account that a certain fraction of energy may be lost in the switch as a result of comparatively high values of its resistance and inductance. Therefore, the high-voltage switch used in this work was a specially developed gas-filled spark gap with a resistance and self-inductance lower than those of a RU-65 standard spark gap [7].

The distance between the main electrodes in the discharge chamber was 2.7 cm, the length of the active part was 59 cm, and the discharge width determined from the light spot was ~ 1.0 cm. The active volume was thus 160 cm^3. The automatic UV preionisation was accomplished by two rows of spark gaps arranged on a side of one of the main electrodes. The discharge chamber was sealed with plane–parallel MgF_2 plates, one of which served as the resonator output mirror. The second mirror was an external dielectric mirror with a reflectivity of 99 % at a lasing wavelength of 248 nm. The optical length of the resonator was 120 cm.

3. Results

To determine the optimal pump intensities for a KrF laser on a He–Kr–F_2 mixture, we have developed a theoretical model of the pump system and constructed a kinetic model of the processes occurring in the active medium of this laser. The results of this analysis were compared to the results of our experiments.

In the numerical simulation of the discharge and lasing dynamics, the kinetic equations for the components of the mixture were solved jointly with an equation for the laser supply circuit and the Boltzmann equation for the energy distribution function for electrons in an electric field [9]. The scheme of kinetic processes that was used in this simulation included 74 plasmachemical reactions (Table 1). The rate constants of the processes of interactions between the components of the gaseous mixture (He, Kr, and F_2) and electrons were calculated from the Boltzmann equation. The cross sections of elastic and inelastic collisions of electrons with He and Kr atoms were taken from [17–19] and [18, 20–23], respectively. The cross sections of the interactions of electrons with F_2 molecules are taken from [24].

The pump system was calculated for the circuit of the LC inverter with automatic UV preionisation and the low-inductance discharge circuit (Fig. 1). In this work, the inductance of the main circuit of the pump system was increased by introducing an additional inductor L_5 that was installed in the circuit section between the LC inverter and the low-inductance discharge circuit, as shown in Fig. 1. This section is in essence a current return conductor. In this case, the total inductance of the LC inverter is determined by $L = L_2 + L_5$. This method of matching the parameters of the LC inverter to the parameters of the discharge circuit was already tested by us in studies of the KrF laser in [7]. However, since the data on the influence of the additional inductance L_5 on the lasing efficiency of this laser were insufficient, the operation of the pump system with L_5 was not described in detail in [7].

To analyse the pump system theoretically, preliminary calculations of the output-energy-optimised composition and the total pressure of the active gaseous medium were performed. The calculation results have shown that the ratio of the mixture components He : Kr : F_2 = 89.8 : 10 : 0.2 is optimal and coincides well with the experimental results from [7]. The total pressure depended on the charging voltage and increased from 2.1 to 2.9 atm in the range of 18–26 kV. The time dependences of the voltage pulses across C_1, C_2, and C_3 and the current pulses through them were calculated for the above parameters of the active medium at various charging voltages and coincided to a 10 % accuracy with current and voltage oscillograms obtained experimentally across these capacitors. Hence, the theoretical model of operation of the KrF laser on a He–Kr–F_2 mixture correctly described the experimental results of studies of the pump and laser-radiation parameters.

The developed model was used to study theoretically the effect of the inductor L_5 on the KrF-laser output energy. The results of this study (Fig. 2) show that the L_5 value strongly affects the output energy but lies within a certain narrow range (80–100 nH). The theoretical analysis has shown that the L_5 inductance affects the voltage U at which the discharge gap is broken down and on the total current J

Table 1.

Reaction number	Reaction	Rate constant/$cm^3\ s^{-1}$; $cm^6\ s^{-1}$	References
1	$He + e \rightarrow He^* + e$	Calculated from the Boltzmann equation	
2	$He + e \rightarrow He^+ + e + e$	– " –	
3	$Kr + e \rightarrow Kr^* + e$	– " –	
4	$Kr + e \rightarrow Kr^{**} + e$	– " –	
5	$Kr + e \rightarrow Kr^+ + e + e$	– " –	
6	$Kr^* + e \rightarrow Kr^+ + e + e$	– " –	
7	$Kr^{**} + e \rightarrow Kr^+ + e + e$	– " –	
8	$Kr^* + e \rightarrow Kr^{**} + e$	– " –	
9	$Kr^{**} + e \rightarrow Kr^* + e$	– " –	
10	$F_2 + e \rightarrow F_2(v) + e$	– " –	
11	$F_2 + e \rightarrow F_2^* + e$	– " –	
12	$F_2 + e \rightarrow F_2^+ + 2e$	– " –	
13	$F_2 + e \rightarrow F + F^-$	– " –	
14	$F_2 + e \rightarrow F + F + e$	– " –	
15	$Kr^+ + Kr + He \rightarrow Kr_2^+ + He$	$10^{-32} T^{-0.75}$	[10]
16	$Kr^+ + Kr + Kr \rightarrow Kr_2^+ + Kr$	$1.5 \times 10^{-32} T^{-0.75}$	[10]
17	$Kr^* + Kr + He \rightarrow Kr_2^* + He$	$10^{-33} T^{-0.75}$	[10]
18	$Kr^{**} + Kr + He \rightarrow Kr_2^* + He$	$10^{-33} T^{-0.75}$	[10]
19	$Kr^* + Kr + Kr \rightarrow Kr_2^* + Kr$	$3 \times 10^{-33} T^{-0.75}$	[10]
20	$Kr^{**} + Kr + Kr \rightarrow Kr_2^* + Kr$	$3 \times 10^{-33} T^{-0.75}$	[10]
21	$He^+ + He + He \rightarrow He_2^+ + He$	1.1×10^{-31}	[9]
22	$He^* + He + He \rightarrow He_2^* + He$	0.43×10^{-33}	[9]
23	$Kr + He^* \rightarrow Kr^+ + He + e$	2×10^{-10}	[10]
24	$Kr + He^+ \rightarrow Kr^+ + He$	10^{-11}	[10]
25	$Kr + He_2^* \rightarrow Kr^+ + 2He + e$	3.7×10^{-10}	[10]
26	$Kr + He_2^+ \rightarrow Kr^+ + 2He$	2×10^{-11}	[10]
27	$Kr^* + Kr^* \rightarrow Kr_2^+ + e$	10^{-9}	[11]
28	$Kr^{**} + Kr^{**} \rightarrow Kr_2^+ + e$	10^{-9}	[11]
29	$Kr^* + F_2 \rightarrow KrF^* + F$	10^{-9}	[11]
30	$Kr^{**} + F_2 \rightarrow KrF^* + F$	10^{-9}	[11]
31	$Kr^* + F^- \rightarrow KrF^* + e$	5.4×10^{-9}	[11]
32	$Kr^{**} + F^- \rightarrow KrF^* + e$	5.4×10^{-9}	[11]
33	$Kr_2^* + F_2 \rightarrow Kr_2F^* + F$	2.1×10^{-10}	[10]
34	$Kr_2^* + F^- \rightarrow Kr_2F^* + e$	3×10^{-9}	[10]
35	$Kr_2^+ + F^- \rightarrow KrF^* + Kr$	$4 \times 10^{-9} T^{-1.5}$	[10]
36	$F + He + e \rightarrow F^- + He$	$6.6 \times 10^{-34} T_e^{-1.5}$	[10]
37	$KrF^* + Kr \rightarrow Kr + Kr + F$	8.6×10^{-12}	[10]
38	$KrF^* + F_2 \rightarrow Kr + 3F$	5×10^{-10}	[10]
39	$KrF^* + 2Kr \rightarrow Kr_2F^* + Kr$	$4 \times 10^{-32} T_e^{-0.75}$	[10]
40	$KrF^* + Kr + He \rightarrow Kr_2F^* + He$	$2 \times 10^{-32} T_e^{-0.75}$	[10]
41	$KrF^* + Kr + He \rightarrow F + 2Kr + He$	5×10^{-31}	[11]
42	$KrF^* + 2He \rightarrow F + Kr + 2He$	5×10^{-32}	[11]
43	$KrF^* + F^- \rightarrow Kr + 2F + e$	2×10^{-9}	[10]
44	$KrF^* + e \rightarrow Kr + F + e$	2×10^{-7}	[10]
45	$KrF^* + e \rightarrow Kr^+ + F + 2e$	$4 \times 10^{-5} T_e^{-3} \exp(-9/T_e)$	[10]
46	$Kr_2F^* + Kr \rightarrow KrF^* + 2Kr$	$3.5 \times 10^{-3} T^{0.75} \exp(-0.49/T)$	[10]
47	$Kr_2F^* + He \rightarrow KrF^* + Kr + He$	$1.7 \times 10^{-3} T^{0.75} \exp(-0.49/T)$	[10]
48	$Kr_2F^* + F_2 \rightarrow 2Kr + 3F$	2×10^{-10}	[10]
49	$Kr_2F^* + F^- \rightarrow 2Kr + 2F + e$	2.4×10^{-9}	[10]
50	$Kr_2F^* + e \rightarrow 2Kr + F + e$	2.3×10^{-7}	[10]
51	$Kr_2F^* + e \rightarrow Kr_2^+ + F + 2e$	$4 \times 10^{-5} T_e^{-3} \exp(-8.5/T_e)$	[10]
52	$F_2^+ + F^- \rightarrow F_2 + F$	10^{-6}	[10]
53	$Kr^+ + F^- + M \rightarrow KrF^* + M$	Calculated from the Flannery formulas	[13]
54	$Kr_2^+ + F^- + M \rightarrow Kr_2F^* + M$	– " –	[13]
55	$He^+ + F^- + M \rightarrow He^* + F + M$	– " –	[14]
56	$He_2^+ + F^- + M \rightarrow 2He + F + M$	– " –	[14]
57	$Kr_2^* + e \rightarrow 2Kr + e$	3×10^{-8}	[10]
58	$He_2^* + e \rightarrow 2He + e$	3.8×10^{-9}	[10]
59	$Kr_2^* + e \rightarrow Kr^* + Kr$	10^{-7}	[11]

See Continuation of Table 1 on the next page.

Reaction number	Reaction	Rate constant/$cm^3\ s^{-1}$; $cm^6\ s^{-1}$	References
60	$He_2^+ + e \rightarrow 2He$	$0.2 \times 10^{-7}(T/T_e)^{0.5}$	[9]
61	$Kr^* + e \rightarrow Kr + e$	2×10^{-8}	[10]
62	$Kr^{**} + e \rightarrow Kr + e$	2×10^{-8}	[10]
63	$He^* + e \rightarrow He + e$	2.6×10^{-9}	[10]
64	$Kr^{**} \rightarrow Kr^* + hv'$	3.4×10^7	[15]
65	$Kr^* + hv \rightarrow Kr^+ + e$	1.3×10^{-19} s	[16]
66	$Kr^{**} + hv \rightarrow Kr^+ + e$	4.5×10^{-18} s	[16]
67	$hv + F^- \rightarrow F + e$	5.6×10^{-18} s	[12]
68	$hv + F_2 \rightarrow 2F + e$	1.5×10^{-20}	[12]
69	$hv + Kr_2^+ \rightarrow Kr^+ + Kr^*$	1.6×10^{-18} cm^2	[12]
70	$hv + Kr_2F^* \rightarrow Kr + F + Kr^+ + e$	1.6×10^{-18} s	[12]
71	$hv + KrF^* \rightarrow KrF(X) + 2hv$	2.53×10^{-16} s	[12]
72	$KrF^* \rightarrow KrF(X) + hv$	$1/(7 \times 10^{-9})$	[10]
73	$KrF(X) \rightarrow Kr + F$	$1/(2 \times 10^{-9})$	[10]
74	$hv + KrF(X) \rightarrow KrF^*$	2.53×10^{-16} s	[10]

Note: (M) buffer gas; (X) ground state of an excimer molecule; T and T_e are measured in kelvins.

through the active medium. In addition, as L_5 increases, the delay Δt between the onsets of the UV preionisation pulse and the current J pulse through the gaseous mixture also increases. This has a positive effect on both the volume-discharge homogeneity and the efficiency of energy deposition into the active medium. The results of the theoretical analysis were confirmed experimentally. When the additional inductor L_5 was absent, the self-inductance of the LC circuit was ~ 30 nH. This inductance was initially minimised (this is a usual tendency in designing the pump systems for excimer lasers) and was obtained as a result of a special arrangement of the storage capacitors C_1, C_2 and switch R_1 around the low-inductance circuit formed by the discharge chamber and storage C_3.

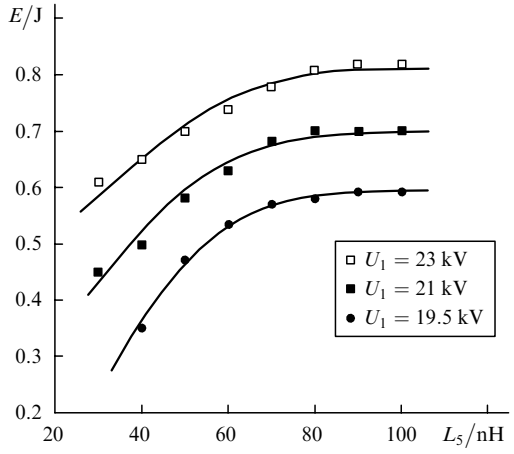

Figure 2. Calculated laser output energy E as a function of the L_5 inductance at various charging voltages U_1.

Figure 3 shows the experimental dependences of the voltage U across the discharge gap, the total current J through it, and the delay time Δt on the introduced inductance L_5. As L_5 increases to 80 nH, all these parameters increase considerably, and between 80 and 100 nH this process saturates. Measurements of the output energy E yielded a similar dependence on the L_5 value. At $L_5 \geqslant 100$ nH, a decrease of both the lasing energy and the total laser efficiency was observed. The optimal L_5 value is thus 80–100 nH. In subsequent studies, we used $L_5 = 80$ nH.

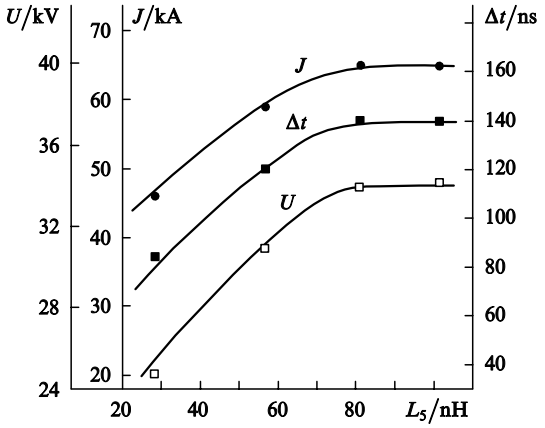

Figure 3. Voltage U across the discharge gap, the discharge current J, and the delay time Δt between the UV preionisation onset and the breakdown of the discharge gap as functions of the L_5 inductance at a charging voltage $U_1 = 21$ kV.

Under such conditions, virtually linear dependences of the voltage U across the discharge gap and the total current J through it on the charging voltage U_1 were obtained experimentally (Fig. 4). They corresponded to a linear dependence of the pump intensity W on the charging voltage

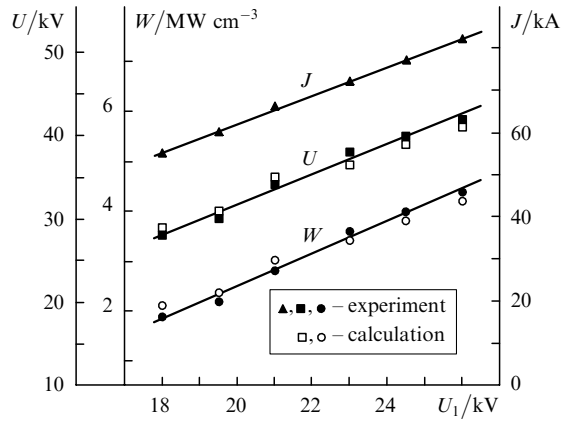

Figure 4. Calculated and experimental dependences of the voltage U across the discharge gap, the discharge current J, and the pump intensity W versus the charging voltage U_1 at $L_5 = 80$ nH.

U_1. For the minimum charging voltage $U_1 = 18$ kV, the pump intensity $W = 1.9$ MW cm^{-3}; for $U_1 = 26$ kV, the pump intensity $W = 4$ MW cm^{-3}.

Figure 5 shows the output energy and the total efficiency η for the KrF laser on the He–Kr–F_2 mixture as functions of the charging voltage U_1. One can see that when the charging voltage rises from 18 to 26 kV, the output energy increases from 0.47 J to 1.0 J, while the efficiency changes very slowly from 1.9 % to 2 %.

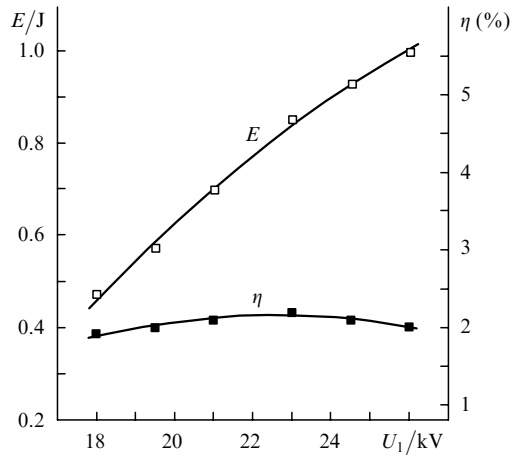

Figure 5. Experimental dependences of the output energy E and the total efficiency η of the KrF laser on the charging voltage U_1 for the active medium with a composition He : Kr : F_2 = 89.8 : 10 : 0.2 at $L_5 = 80$ nH.

The maximum output energy at $\eta = 2$ % is 1 J. The results of studies allowed us to determine the optimal values of the pump intensity for the KrF laser on the He–Kr–F_2 mixture. Figure 6 shows the total lasing efficiency as a function of W. Obtaining the maximum efficiency under such excitation conditions requires a pump intensity of 3–4 MW cm^{-3}, which is higher than the optimal values obtained in [4, 5].

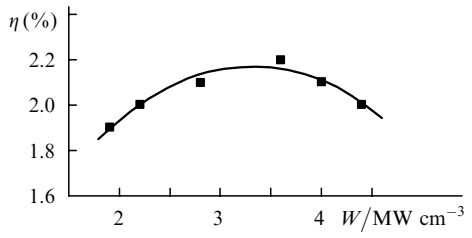

Figure 6. Total efficiency η of the KrF laser versus the pump intensity W for the active medium with a composition He : Kr : F_2 = 89.8 : 10 : 0.2 at $L_5 = 80$ nH.

4. Discussion

To achieve high values of the efficiency and output energy of the KrF laser on the He–Kr–F_2 mixture, we have proposed to increase the pump intensity to 4.0 MW cm^{-3}; this was realised by increasing the inductance of the main circuit in the pump system by including an additional inductor L_5 in the circuit (Fig. 1).

In our opinion, the effect of this inductor on the efficiency and output energy of the KrF laser on the He–Kr–F_2 mixture is as follows. After the switch in the LC inverter is turned on and the voltage polarity at C_1 is reversed, the energy of the capacitors C_1 and C_2 is transferred to C_3 of the low-inductance circuit. It is obvious that the efficiency of the energy transfer from C_1 and C_2 of the LC-inverter circuit to C_3 is a parameter that determines the efficiency of operation of the pump system. The transfer efficiency depends on the L_2 value; the lower this inductance, the higher the capacitors' charge-exchange rate and the lower the energy lost in this processes. However, when the capacitor C_3 subsequently charges to the breakdown voltage of the gap between the main electrodes, it is broken down, its discharge begins, and the energy from C_3 is transferred to the active medium and also returns to the LC inverter. This leads to a loss in the energy deposited into the discharge. This loss can be reduced by increasing the inductance of the main discharge circuit by adding the inductor L_5, which in aggregate with L_2 limits the return current from C_3 to the capacitors C_1 and C_2 of the LC inverter. The L_5 inductance cannot obviously be high, since this decreases the efficiency of the energy transfer from C_1 and C_2 to C_3; however, it cannot be lower than a certain value (80 nH in our case) in order to prevent the reverse process. This conclusion is confirmed by a theoretical analysis of the current pulses through these capacitors and voltages across them at the instant of C_3 discharge for different L_5 values. As a result, both the voltage across the discharge gap and the current through it increase, and the energy deposited into the active medium thus also increases. As a consequence, the output energy and efficiency of the KrF laser on the He–Kr–F_2 mixture also increase.

When the L_5 inductance increases to 80 nH, the delay of the discharge-gap breakdown onset relative to the onset of the UV preionisation pulse increases from 90 to 140 ns, which always affects the volume-discharge homogeneity. It was shown in [25, 26] that, when the delay of the main-discharge onset relative to the onset of the UV preionisation pulse changes from 0 to 4000 ns, the maximum output energy of excimer lasers is achieved at $\Delta t = 200 - 300$ ns; this is explained by a combination of the required preionisation intensity and homogeneity determining the space-discharge homogeneity at high pressures. Hence, approaching this range of optimal delays must also result in an increase in the laser output energy and efficiency.

5. Conclusions

We have developed a theoretical model of a KrF gas-discharge excimer laser on a He–Kr–F_2 mixture. A pump system based on an LC inverter with automatic UV preionisation and an additional inductance is created. The effect of the excitation parameters on the output energy characteristics of a KrF laser on a He–Kr–F_2 mixture is studied theoretically and experimentally. To enhance its output energy and efficiency, it is proposed to increase the pump intensity by using an additional inductance of ~ 80 nH in the LC inverter. It is shown that the maximum output energies are achieved at a specific pump intensity of ~ 4.0 MW cm^{-3}. The maximum output energy for the He–Kr–F_2 mixture at a charging voltage of 26 kV is 1.0 J, which corresponds to a pulse power of > 40 MW for a pulse FWHM of 24 ns.

References

1. Miyazaki K., Hasama T., Yamada K., et al. *J. Appl. Phys.*, **60**, 2721 (1986).
2. Borisov V.M., Bragin I.E., Vinokhodov A.Yu., Vodchits V.A. *Kvantovaya Elektron.*, **22**, 533 (1995) [*Quantum Electron.*, **25**, 507 (1995)].
3. Borisov V.M., Borisov A.V., Bragin I.E. *Kvantovaya Elektron.*, **22**, 446 (1995) [*Quantum Electron.*, **25**, 421 (1995)].
4. Armandillo E., Bonanni F., Grasso G. *Opt. Commun.*, **42** (1), 63 (1982).
5. Watanabe S., Endoh A. *Appl. Phys. Lett.*, **41** (9), 799 (1982).
6. Nodomi R., Ueda Y., Sajiki K., Nakajima S., Watanabe M., Watanabe S. *IEEE J. Quantum Electron.*, **27** (3), 441 (1991).
7. Zhupikov A.A., Razhev A.M. *Kvantovaya Elektron.*, **25**, 687 (1998) [*Quantum Electron.*, **28**, 667 (1998)].
8. Razhev A.M., Zhupikov A.A., Kargapol'tsev E.S. *Kvantovaya Elektron.*, **34**, 95 (2004) [*Quantum Electron.*, **34**, 95 (2004)].
9. Lo D., Shchedrin A.I., Ryabtsev A.V. *J. Phys. D*, **29**, 43 (1996).
10. Artemov M.S., Bunkin F.V., et al. *Kvantovaya Elektron.*, **13**, 2191 (1986) [*Sov. J. Quantum Electron.*, **16**, 1448 (1986)].
11. Borisov V.M., Vysikailo F.I., et al. *Kvantovaya Elektron.*, **12**, 1196 (1985) [*Sov. J. Quantum Electron.*, **15**, 791 (1985)].
12. McDaniel I., Nigan W. (Eds) *Gas Lasers* (New York: Acad. Press Publishing, 1980).
13. Flannery M.R., Yang T.P. *Appl. Phys. Lett.*, **33**, 574 (1978).
14. Flannery M.R., Yang T.P. *Appl. Phys. Lett.*, **32**, 327 (1978).
15. Dzierzega K., Volz U., Nave G., et al. *Phys. Rev. A*, **62**, 022505 (2000).
16. Hyman H.A. *Appl. Phys. Lett.*, **31**, 14 (1977).
17. http://www.kinema.com/sigmalib.dat
18. Rejoub R., Lindsay B.G., Stebbings R.F. *Phys. Rev. A*, **65**, 042713 (2002).
19. Saha H.P. *Phys. Rev. A*, **40**, 2977 (1989).
20. Dasgupta A., Bartschat K., Vaid D., et al. *Phys. Rev. A*, **64**, 052710 (2001).
21. Chilton J.E., Stewart M.D., Lin C.C. *Phys. Rev. A*, **62**, 032714 (2000).
22. Hyman H.A. *Phys. Rev. A*, **20**, 855 (1979).
23. Hyman H.A. *Phys. Rev. A*, **18**, 441 (1978).
24. Hayashi M., Nimura T. *J. Appl. Phys.*, **54**, 4879 (1983).
25. Hsia J. *Appl. Phys. Lett.*, **30** (2), 101 (1977).
26. Luches A., Nassisi V., Perrone M.R. *J. Phys. E: Scientific Instruments*, **20** (8), 1015 (1987).